REPORT DOCUMENTATION PAGE

Form Approved
OMB NO. 0704-0188

1. AGENCY USE ONLY (Leave Blank)	2. REPORT DATE	3. REPORT TYPE AND DATES COVERED
	May, 2005	Peer Reviewed Reprint

4. TITLE AND SUBTITLE
"Photonic Crystal Nanocavity Arrays,"

5. FUNDING NUMBERS
DAAD19-03-1-0199

6. AUTHOR(S)
Hatice Altug and Jelena Vuckovic,

7. PERFORMING ORGANIZATION NAME(S) AND ADDRESS(ES)
Ginzton Laboratory, Stanford University, Stanford, CA 94305-4088

8. PERFORMING ORGANIZATION REPORT NUMBER

9. SPONSORING / MONITORING AGENCY NAME(S) AND ADDRESS(ES)
U. S. Army Research Office
P.O. Box 12211
Research Triangle Park, NC 27709-2211

10. SPONSORING / MONITORING AGENCY REPORT NUMBER
45116.65-PH-MUR

11. SUPPLEMENTARY NOTES
The views, opinions and/or findings contained in this report are those of the author(s) and should not be construed as an official Department of the Army position, policy or decision, unless so designated by other documentation.
Published in *IEEE LEOS Newsletter,* vol. 20, No. 2, pp. 4-11, April 2006 (Invited article)

12 a. DISTRIBUTION / AVAILABILITY STATEMENT
Approved for public release; distribution unlimited.

12 b. DISTRIBUTION CODE

13. ABSTRACT (Maximum 200 words)

We recently proposed two-dimensional coupled photonic crystal nanocavity arrays as a route to achieve a slow-group velocity of light in all crystal directions, thereby enabling numerous applications ranging from low-threshold nonlinear optics to improved lasers. In this article, we review some of our recent experimental results on such structures, ranging from the measurement of group velocities below 0.008c to a new type of laser composed of an array of coherently coupled photonic crystal nanocavities. We show that such lasers exhibit a high differential quantum efficiency and output power, together with a low threshold power comparable to those of single photonic crystal cavity lasers. The measured laser efficiency increases faster than the lasing threshold with an increase in the number of coupled cavities and enables single mode lasing with output powers that are two orders of magnitude higher than in single nanocavity lasers.

14. SUBJECT TERMS
photonic crystals, lasers, nanocavity arrays, slow light

15. NUMBER OF PAGES

16. PRICE CODE

17. SECURITY CLASSIFICATION OR REPORT	18. SECURITY CLASSIFICATION ON THIS PAGE	19. SECURITY CLASSIFICATION OF ABSTRACT	20. LIMITATION OF ABSTRACT
UNCLASSIFIED	UNCLASSIFIED	UNCLASSIFIED	UL

Photonic crystal nanocavity arrays

Hatice Altug and Jelena Vuckovic

Abstract

We recently proposed two-dimensional coupled photonic crystal nanocavity arrays as a route to achieve a slow-group velocity of light in all crystal directions, thereby enabling numerous applications ranging from low-threshold nonlinear optics to improved lasers. In this article, we review some of our recent experimental results on such structures, ranging from the measurement of group velocities below 0.008c to a new type of laser composed of an array of coherently coupled photonic crystal nanocavities. We show that such lasers exhibit a high differential quantum efficiency and output power, together with a low threshold power comparable to those of single photonic crystal cavity lasers. The measured laser efficiency increases faster than the lasing threshold with an increase in the number of coupled cavities and enables single mode lasing with output powers that are two orders of magnitude higher than in single nanocavity lasers.

Introduction

It has been first predicted by Purcell that spontaneous emission is not inherent to an emitter but can be changed if its electromagnetic environment is modified [1]. Optical microcavities can be used to enhance the spontaneous emission rate as they can dramatically increase electromagnetic density of states (DOS) with respect to free space (also known as the Purcell effect). This effect can be used to improve the speeds of lasers and to increase the fraction of spontaneously emitted photons that are coupled into a single cavity mode (denoted as the spontaneous emission-coupling factor β), thereby enabling lasers with low lasing threshold powers [2]. The spontaneous emission rate enhancement is directly proportional to the cavity quality factor (Q) and inversely proportional to the cavity mode volume (V_{mode}). In recent years, photonic crystal [3-4] nanocavities have been extensively studied for spontaneous emission control due to their very large Q/V_{mode} ratios [5-6]. In fact, photonic crystal nanocavities have been explored to realize low threshold lasers [7-9]. Unfortunately, the output power levels of such lasers are extremely low (a few nW), below the levels needed for many practical applications.

To overcome these problems, we recently proposed [10] and experimentally demonstrated [11-12] two-dimensional (2D) coupled photonic crystal (PhC) nanocavity array structures, which enable very large density of optical states. We employed them to improve the performance of photonic crystal lasers [13], such as improving their output power and reducing threshold. Our experimental results are summarized in this paper.

EDWARD L. GINZTON LABORATORY, STANFORD UNIVERSITY,
STANFORD, CA 94305-4088
ALTUG@STANFORD.EDU, JELA@STANFORD.EDU

Theoretical Analysis of 2D PhC Coupled Cavity Arrays

A 2D coupled nanocavity array is formed by tiling nanocavities in two dimensions inside a photonic crystal, such as a 2D PhC slab of square lattice (Fig. 1). When combined into a two-dimensional network, defect modes of individual cavities form coupled defect bands located inside the photonic bandgap [10]. In particular, the coupled arrays in the square lattice photonic crystal exhibit three coupled TE-like bands: monopole, dipole, and quadrupole. Their z-components (the only nonzero components) of the magnetic field at the center of the PhC slab are shown in Fig. 2. The band diagram shown in Fig. 2 is simulated by three-dimensional finite-difference time-domain (3D FDTD) method. Since the unit cell of the coupled cavity array is three times bigger than the unit cell of the original square lattice, square lattice band diagram is folded three times in order to plot it together with the band diagram of the cavity array structure. Dielectric and air bands are shaded in gray.

The coupled dipole bands originate from the doubly degenerate dipole mode; two sub-bands corresponding to the coupled x- and the y-dipoles split away from the Γ point in the ΓX direction, while one degenerate diagonal dipole band is observed in the ΓM direction. By being linearly polarized, this band is useful to control polarization state of light. In fact, in our previous works we used it for construction of miniaturized polarizing components and as sensors for refractive index changes [11]. Conversely, the coupled quadrupole band is flat (which corresponds to large DOS) in all crystal directions, as it originates from the non-degenerate quadrupole mode with a large in-plane Q-factor that has four-fold symmetric radiation pattern. The first derivative of the dispersion diagram, $\omega(k)$, gives the group velocity. Therefore a flat band corresponds to a reduction in the group velocity of light and a consequent increase in the light-matter interaction time. Thus, coupled quadrupole band is suitable to build lasers with very low threshold powers.

Measuring Group Velocity Reduction:

We experimentally demonstrated the predicted group velocity reduction by measuring the dispersion diagram of the coupled cavity array fabricated in silicon (structures shown in Fig. 1 and measured band diagram in Fig. 3). The size of the device is 100μm×100μm (consisting of 3600 coupled nanocavities). We used transmission spectrum with plane wave excitation at various incidence angles, polarizations and

wavelengths to determine band diagram, and were able to probe half of the ΓX and ΓM directions shown in Fig. 2 [12]. Figs. 3a and 3b represent the measured band diagrams in the ΓX directions for x- and y-dipoles, respectively. The dark blue stripes located between 1545-1565nm in these figures correspond to the positions of the coupled dipole bands. As expected from theory (Fig. 2), we obtained the flat x-dipole band and the non-flat y-dipole band in the ΓX direction. The coupled quadrupole band has not been observed because its overlap with the plane-wave excitation is zero (but we have been able to observe it by non-plane wave excitation [12]).

Once we obtained the band diagram, we could estimate the group velocity reduction from its first derivative. As it can be seen from the measured band diagrams, the location of the x-dipole mode is not changing at different k-points (tilt angles), which indicates that the group velocity should be very small. However, based on our experimental resolution in the tilt angle and frequency we set an upper limit for it in all directions to be below:

$$V_{g|max} = \frac{\Delta\omega}{\Delta k} = \frac{\Delta\lambda}{\lambda}\frac{1}{\Delta\theta} \leq 8 \times 10^{-3} c$$

where $\Delta\theta=\pi/180$ is the tilt step in radians, $\Delta\lambda=0.2$nm is wavelength resolution, $\lambda=1564$nm is the resonance wavelength and c is the speed of light in vacuum.

Coupled Nanocavity Array Lasers

By fabricating same structures in an active material, we can build lasers with significantly improved output powers (resulting from coherent cavity coupling) compared to single photonic crystal cavity lasers, but with comparable threshold values. An illustration of such a laser is shown in Fig. 4a. To demonstrate lasing, we fabricated nanocavity arrays in InP laser material system [13]. The active region contains four InGaAsP quantum wells (QWs) with a peak photoluminescence emission wavelength of 1560nm (Fig. 5). PhC parameters are the free-standing membrane thickness (d) of 280nm, periodicity (a) of 500nm, and the hole radius (r) tuned from 160nm to 230nm to change the resonance frequency of cavities. For comparison, single cavity lasers are also fabricated on the same chip, with the same parameter range (Fig. 4c). With these parameters, the quadrupole mode frequency calculated by FDTD falls within the gain linewidth.

The coupled PhC nanocavity array lasers with sizes ~15μm are optically pumped at room temperature using a confocal microscope with 0.6 NA objective lens. The pump is a pulsed diode laser at 808nm (20ns long with 1% duty cycle) with 15-20μm spot size. Emitted light is coupled to an optical spectrum analyzer. To compare the performance of the coupled cavity array lasers to that of single nanocavity lasers (with size ~4μm), a similar setup with a beam spot size of ~5μm is used. Single mode lasing is observed from coupled nanocavity array lasers (spectrum is shown in Fig. 5). The lasing wavelength matches that of the phase-coupled quadrupole mode at the Γ-point calculated by FDTD.

The profile of the lasing modes from a single cavity taken

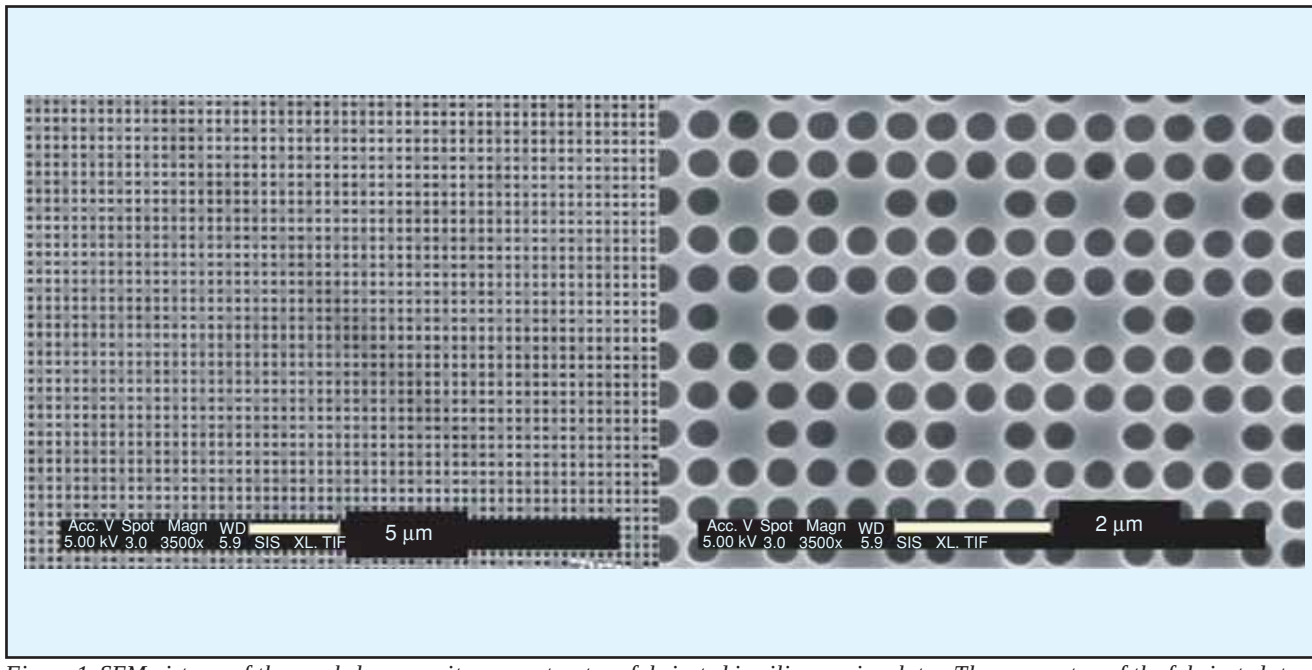

Figure 1. SEM pictures of the coupled nanocavity array structure fabricated in silicon on insulator. The parameters of the fabricated structures are: the PhC periodicity a = 490 nm, the hole radius r = 190nm, the slab thickness d = 275 nm, and the coupled cavity array unit cell dimensions A×A = 3a×3a (i.e., two PhC layers are inserted between tiled nanocavities).

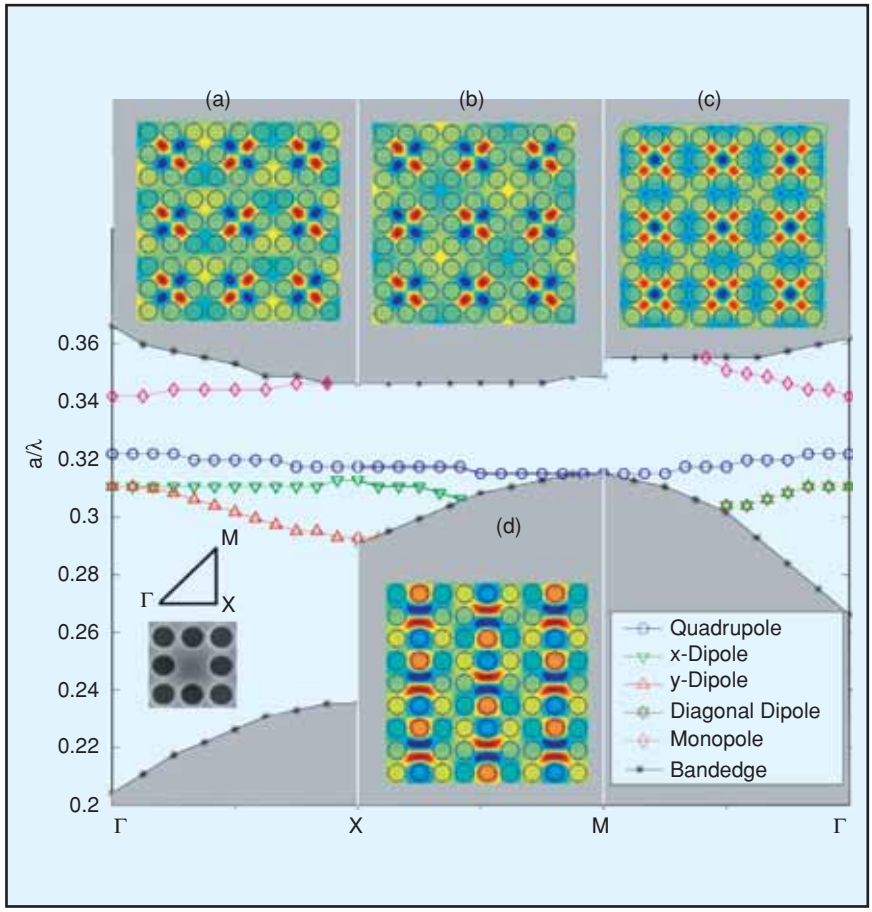

Figure 2. Band diagram of 2D coupled cavity array structure (shown in Fig. 1) for TE-like modes. Dielectric and air bands of the original square lattice are folded three times separately in ΓX, XM and ΓM and shaded in gray. Magnetic field pattern along the z-direction for: (a) quadrupole mode at X point; (b) quadrupole mode at M point; (c) monopole mode at Γ point; (d) x-dipole mode at X point. Unit cell in real space and location of high symmetry points in the reciprocal space are also shown in the inset.

with an infrared-camera is shown in Fig. 6a. It clearly shows the four-fold symmetry of the quadrupole mode. At the center of the square, there is a strong field localization, corresponding to the location of the single defect. The radiation profile is simulated by the FDTD method, by calculating the time averaged Poynting vector in the vertical direction. The radiation patterns at a plane ~1µm above the structure is very similar to the experimentally measured field patterns. Due to poor sensitivity of the IR-camera, it was difficult to observe far field emission pattern of the lasers made in InP. However with same laser structures fabricated in GaAs (with emission wavelength at 940nm) we have been able to capture far field pattern with highly sensitive silicon camera (Fig. 6b). The pattern clearly demonstrated coherently coupled lasing action. Here, the lasing occurred from dipole mode due to better overlap of dipole band with the gain medium.

Coupled nanocavity array lasers with different *r*/*a* ratios have been tested and Fig. 7a shows the measured light-out/light-in (LL) curve of one of them (blue). We have observed single-mode lasing at 1534nm with a threshold peak pump power of ~2.4mW. Several single cavity structures with different *r*/*a* have also been tested. The LL-curve of one of them (with *r*/*a*≈0.4) is shown

Optiwave

INTRODUCING

MAX

THE REVOLUTIONARY HYBRID FDTD SIMULATION WORKSTATION

CLUSTER COMPUTING POWER. WITHOUT THE CLUSTER.

www.optiwave.com

OptiSystem Optical Communication System Design	**OptiFDTD** Time-Domain Photonics Simulation Design	**OptiFDTDMAX** FDTD simulation workstation
OptiBPM Waveguide Optics Modeling Tools	**OptiGrating** Integrated and Fiber Optical Gratings Design	**OptiFiber** Optical Fiber Design

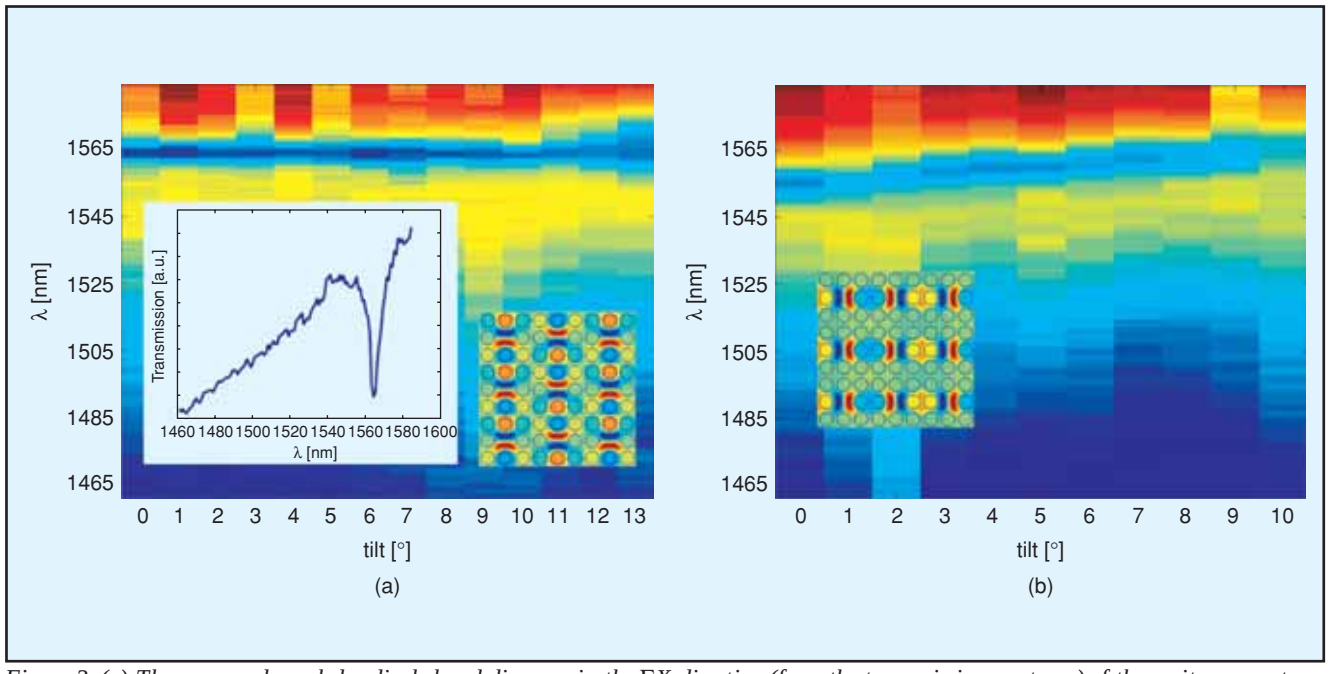

Figure 3. (a) The measured coupled x-dipole band diagram in the ΓX direction (from the transmission spectrum) of the cavity array structure from Fig. 1. The dark blue stripe is the location of the coupled band. The horizontal axis is the tilt angle of the sample relative to excitation beam, which corresponds to different k_x-values; the vertical axis is the wavelength. The insets show the transmission spectrum at 0° tilt (at the Γ point), and the magnetic field (B_z) pattern of the coupled x-dipole mode at the X-point. (b) The measured band diagram for the coupled y-dipole band. The inset shows the magnetic field (B_z) pattern at the X point.

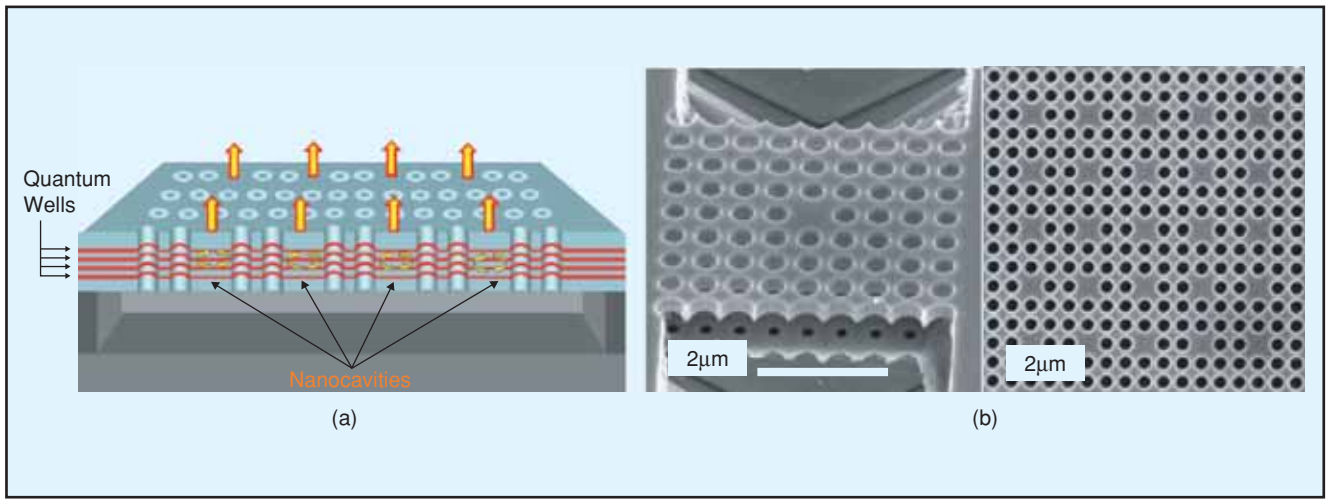

Figure 4. (a) Schematic configuration of the coupled photonic crystal nanocavity array laser structure. (b) SEM pictures of a fabricated single PhC cavity laser and a coupled PhC cavity array laser in InGaAsP-based material. The coupled array consists of 81 cavities (9x9) with two layers of photonic crystal in between.

in Fig. 7 (red). The parameters of this cavity and therefore the emission wavelength at 1543nm are quite similar to the coupled cavity array laser. The threshold peak pump power of the single cavity laser is around ~320μW. The measured lasing threshold of coupled photonic crystal nanocavity arrays is about 10 times larger than for a single cavity. On the other hand, the measured 20-fold increase in differential quantum efficiency (DQE, defined as the slope of the LL-curve above threshold [14]) of the cavity array is larger than the increase in threshold, implying that a higher output power can be extracted per nanocavity in a coupled cavity array laser in comparison to a single nanocavity laser. In fact, the maximum power achieved from our coupled cavity array laser is greater than 12 μW, which is about 100 times larger than a single cavity laser (Fig. 7a).

Coherent coupling of VCSELs has also been previously investigated to improve laser output powers [15-17]. However, since it is very challenging to control the uniformity of the VCSEL arrays and the coupling between individual lasers, phase-locked lasing is only observed from small number of coupled VCSELs [16]. With photonic crystal nanocavity arrays, we can control both the uniformity and the coupling very precisely. As we indicated above, in silicon

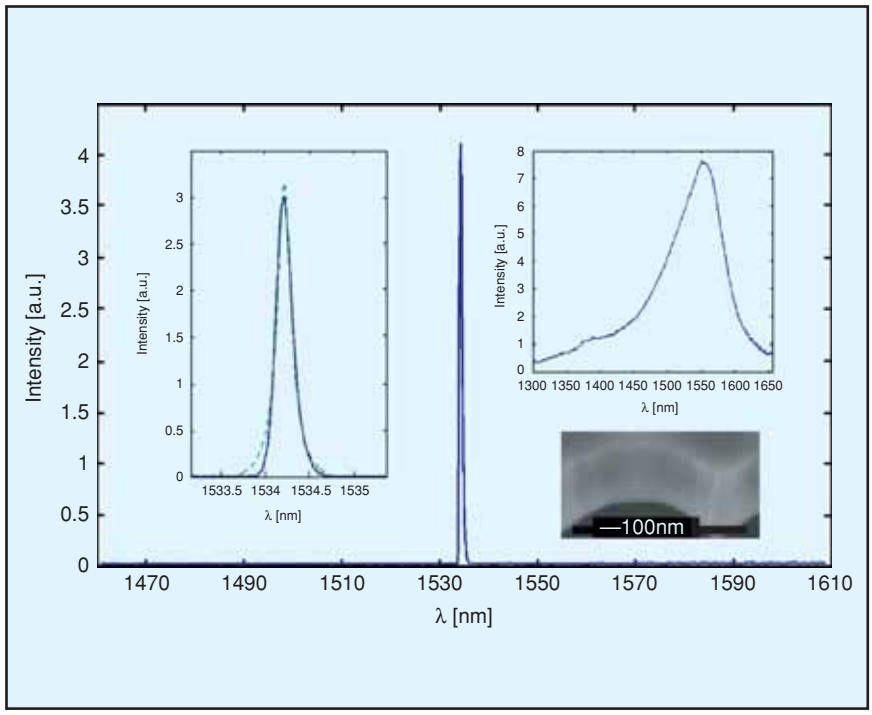

Figure 5. Spectrum of the coupled cavity array laser with a peak at 1534nm. The inset on the left shows the zoomed-in portion of the spectrum fitted with a Lorentzian (green dashed curve) of 0.23nm linewidth. The inset on the right shows the QW photoluminescence from unprocessed wafer (QWs shown on the SEM image).

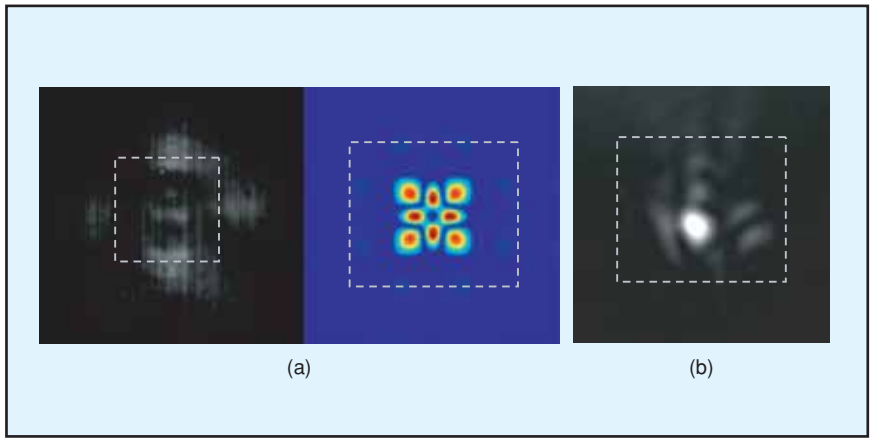

Figure 6. (a) The IR-camera image (left) and the simulated time-averaged Poynting vector in the vertical direction (right) of the lasing mode for a single cavity laser. The size of the structure is indicated by the dashed square. (b) Far field image of a coherently coupled nanocavity array laser. The size of the cavity array laser is indicated by dashed square.

we have able to construct very uniform structures consisting of 3600 coupled PhC nanocavities [12]. Moreover, in our laser each cavity occupies an area of only $1.5\mu m^2$ (much smaller than a typical VCSEL), implying that an ultra-dense packing is achievable with coupled PC nanocavities lasers, which can also enable higher output powers.

By fitting laser rate equations with the typical bulk InGaAsP QW parameters [18] to the measured LL-curves (Fig. 7b), we obtain a range of β values [0.09-0.15] and [0.05-0.09] for single and coupled cavity array laser, respectively. These values are already two orders of magnitude higher than those of VCSELs, which is typically less than 10^{-3}, indicating that the cavity effects in photonic crystal are significant [14].

Laser Differential Quantum Efficiency Improvement

Although we have 81 available cavities in the array, it is expected that not all of them are lasing together, due to fabrication imperfections. In order to estimate the number of coherently coupled cavities, n_c, we have solved rate equations [14] for n_c changing from 10, 40 to 70 and compare them with the solution for a single cavity laser (Fig. 7b). In equations, we set the ratio of pumped active volume (V_a) of the cavity array to that of a single cavity as 10, which is estimated from the size of the pumping beam. When we compare the experimental and theoretical curves shown in Fig. 7a and 7b, respectively, we estimate that a majority of available 81 cavities is actually coherently coupled.

The reason for the DQE improvement in coupled cavity array laser comes from two effects [13]. First one is due to cavity effects. Because of non-negligible β values, an increase in V_{mode} reduces the loss and thus increases DQE. Second effect comes from more efficient pumping. In PhC nanocavity array lasers, the pumped active volume V_a increases slower than the mode volume V_{mode} with an increase in the number of cavities. Hence, the ratio V_{mode}/V_a is larger for nanocavity array laser than for a single PC cavity laser, leading an increase in DQE. This gives a better overlap between the pumped area and the cavity mode. In a single PC cavity laser, it is extremely difficult to pump only the central cavity region, and the pump also generates carriers inside the mirrors, which do not couple to the lasing mode; hence PhC cavity laser is not pumped efficiently. On the other hand, in a coupled PhC cavity array laser one can pack larger number of lasers more efficiently by reducing the space used as mirrors, and the overlap between the pumped region and the cavity mode is better.

Conclusion

In conclusion, we have proposed 2D coupled photonic crystal nanocavity arrays, and experimentally demonstrated their band diagram, confirming flat, coupled defect bands with group velocities below 0.008c. We have used this structure to improve the output power of photonic

crystal lasers. By coherently coupling photonic crystal nanocavity lasers in ultra-dense arrays, we have shown that the differential quantum efficiencies can be improved dramatically, without sacrificing the low lasing thresholds of single PhC nanocavity lasers. We have measured peak output powers from the PhC laser array that are more than two orders of magnitude higher than in a single PhC cavity laser. Output powers comparable to conventional single mode VCSELs, but at much lower threshold pump powers, can be achieved by coupling even larger numbers of PhC cavities. We expect that such structures can also be directly modulated at high speeds, as a result of a strong localization of light [2], implying that coupled nanocavity arrays can be an effective way to achieve high power and high-speed single mode laser sources.

Acknowledgments

This work has been supported by the MARCO Interconnect Focus Center, NSF ECS-04-24080, and MURI Center for Photonic Quantum Information Systems. The authors would like to thank Dirk Englund for help with measuring the radiation pattern of the coupled cavity array.

References

[1] Purcell, E. Spontaneous emission Probabilities at Radio Frequencies. Phys. Rev. 69, 681 (1946).

[2] Yamamoto, Y. et al. Microcavity semiconductor laser with enhanced spontaneous emission, Phys. Rev. A 44, 657-668 (1991)

[3] Yablonovitch, E., Inhibited spontaneous emission in solid-state physics and electronics. Phys. Rev. Lett. 58, 2059-2062 (1987)

[4] John, S. Strong localization of photons in certain disordered dielectric superlattices. Phys. Rev. Lett. 58, 2486-2489 (1987).

[5] Englund, D., et al. Controlling the Spontaneous Emission rate of Single Quantum Dots in a 2D Photonic Crystal. Phys. Rev. Lett. 95, 013904 (2005).

[6] Song, B. S., et al. Ultra-high-Q photonic double-heterostructure nanocavity. Nature materials 4, 207-210 (2005)

[7] Painter, O., et al. Two-dimensional photonic bandgap defect mode laser. Science 284, 1819–1821 (1999).

[8] Loncar, M., et al. Low-threshold photonic crystal laser. Appl. Phys. Lett. 81, 2680-2682 (2002).

[9] Park, H. G., et. al. Electrically Driven Single-Cell Photonic Crystal Laser. Science 305, 1444-14447 (2004).

[10] Altug, H. & Vuckovic, J. Two-dimensional coupled photonic crystal resonator arrays. Appl. Phys. Lett. 84, 161-163 (2004).

[11] Altug, H. & Vuckovic, J. Polarization control and sensing with two-dimensional coupled photonic crystal microcavity arrays. Opt. Lett. 30, 982-984 (2005)

[12] Altug, H. & Vuckovic, J. Experimental demonstration of the slow group velocity of light in two-dimensional coupled photonic crystal microcavity arrays, Appl. Phys. Lett. 86, 111102 (2005)

[13] Altug, H. & Vuckovic, J. Photonic crystal nanocavity array laser. Optics Express 13, 8820-8828 (2005).

[14] Coldren, L. A. & Corzine S. W. Diode Lasers and Photonic Integrated Circuits. New York: Wiley, 1995

[15] Deppe, D. G., et al. Phase-coupled two-dimensional $Al_xGa_{1-x}As$-GaAs vertical-cavity surface-emitting laser array, Appl. Phys. Lett. 56, 2089-2091 (1990)

[16] Warren, M. E., et al. On-axis far-field emission from two-dimensional phase-locked vertical cavity surface-emitting laser arrays with an integrated phase-corrector, Appl. Phys. Lett., 61, 1484-1486 (1992)

[17] Raftery, J. J., et al. Coherent coupling of two-dimensional arrays of defect cavities in photonic crystal vertical cavity surface-emitting lasers, Appl. Phys. Lett. 86, 201104- (2005)

[18] Baba, T. Photonic crystals and microdisk cavities based on GaInAsP-InP system, IEEE J. Select. Topics Quantum Electron., 3, 808-811 (1997)